



# Beryllium and carbon films in JET following D–T operation

M. Rubel <sup>a,\*</sup>, J.P. Coad <sup>b</sup>, N. Bekris <sup>c</sup>, S.K. Erents <sup>b</sup>, D. Hole <sup>d</sup>, G.F. Matthews <sup>b</sup>,  
R.-D. Penzhorn <sup>c</sup>, Contributors to EFDA-JET work programme

<sup>a</sup> *Alfvén Laboratory, Royal Institute of Technology, Association EURATOM – VR, Teknikringen 31, S-100 44 Stockholm, Sweden*

<sup>b</sup> *JET-EFDA, Culham Science Centre, Association EURATOM – UKAEA-Fusion, Abingdon, Oxfordshire OX14 3DB, UK*

<sup>c</sup> *Tritium Laboratory, Forschungszentrum Karlsruhe, Association EURATOM – FZK, D-76021 Karlsruhe, Germany*

<sup>d</sup> *School of Mathematical and Physical Sciences, Accelerator Laboratory, University of Sussex, BN1 9QH Brighton, UK*

---

## Abstract

After the D–T operation (DTE-1 campaign) at JET a large number of limiter and divertor tiles were dismantled from the torus for ex situ examination. The relative distributions of deuterium, tritium, beryllium and carbon are presented and discussed. Significant asymmetry observed in the distribution of erosion and deposition zones indicates preferential flow of the deuterium background plasma and impurities towards the inner divertor leg. The comparison of the beryllium content on the limiter tiles from the main chamber and the content of this element on the inner divertor tiles clearly proves the beryllium erosion from the main chamber wall and its transport to the divertor. However, no beryllium is detected in the shadowed regions of the divertor where the formation of thick and fuel-rich carbon films occurs. This is interpreted in terms of different mechanisms governing the erosion and transport of Be and C. The results allow a conclusion that the operation with a full beryllium wall would lead to a significantly decreased fuel inventory due to removal of the carbon source.

© 2003 Elsevier Science B.V. All rights reserved.

*PACS:* 52.40.Hf

*Keywords:* Hydrogen inventory; Erosion; Re-deposition; Beryllium; Carbon films; JET

---

## 1. Introduction

The JET tokamak is the only controlled fusion facility experienced in a large-scale simultaneous use of a deuterium-tritium fuel [1,2] and a beryllium coating evaporated on a carbon wall [3,4]. All these elements are going to be adopted in ITER [5]. Therefore, it is essential to gather relevant information regarding the material erosion, its transport and resulting deposition on plasma facing components (PFC) in present day experiments. Studies of PFC have regularly been carried out at JET following each major experimental campaign in order to assess the impact of operation scenarios, wall tempera-

ture and divertor configuration on the surface morphology and fuel inventory. The review has been given in [6].

In recent years, the presence of T and Be has strongly limited the access to the machine. As a consequence, samples of PFC for detailed ex situ studies can only be retrieved using a robotic arm [7] operated remotely during major interventions in the torus. These are primarily connected with the change of the divertor configuration. For the first time the robot was used in 1998 to exchange the MkII-A divertor with the MkII-GB (gas box) and to replace some of the limiter tiles in the main chamber. Many dismantled tiles could then be examined with tritium tracing and surface analysis methods. The aim of this study is to determine the distribution of erosion and deposition zones and, by this, to assess the fuel inventory, material erosion and its transport mechanism.

---

\* Corresponding author. Tel.: +46-8 790 60 93; fax: +46-8 24 54 31.

E-mail address: [rubel@fusion.kth.se](mailto:rubel@fusion.kth.se) (M. Rubel).

## 2. Experimental

After the D–T experiments (DTE1 campaign in 1997) and the operation aiming at the tritium recovery by various clean-up procedures [2] a number of graphite and carbon fibre composite (CFC) tiles were removed from the torus. These included representative samples from the inner guard (six tiles) and poloidal (three tiles)

limiters and the Mk-IIA divertor (10 tiles, i.e. a full poloidal set). The location of tiles in the main chamber is marked on a schematic poloidal cross-section of the torus (Fig. 1(a)), whereas Fig. 1(b) shows a cross-section of the divertor. Preparation of samples, totalling 204 pieces, for further studies was done in the Tritium Laboratory of the Forschungszentrum Karlsruhe, Germany. Two sets (102 pieces each) of cylindrical samples,

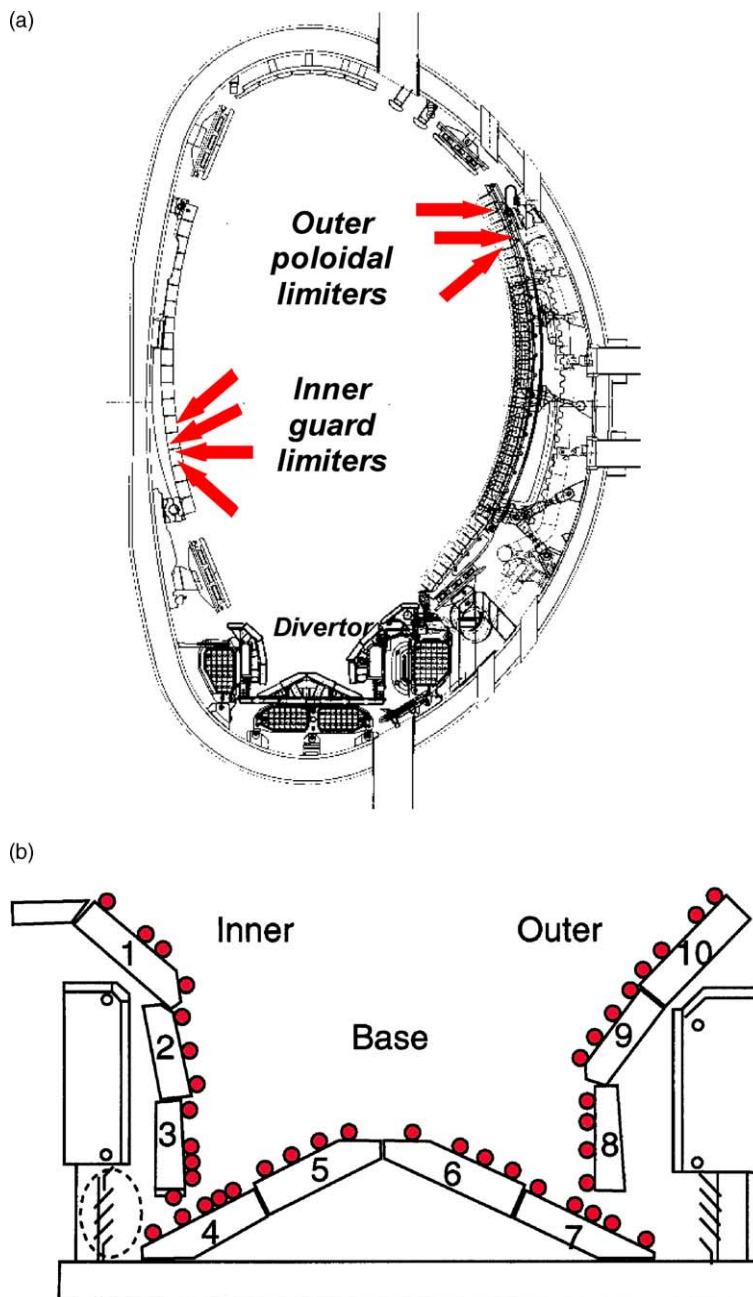


Fig. 1. Schematic cross-section and location of tiles and samples in the JET (a) vessel and the (b) Mk-IIA divertor.

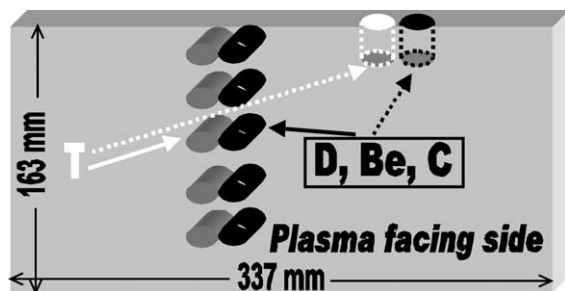


Fig. 2. Sampling procedure for the determination of tritium with a full combustion method and other elements (D, Be, C) by surface analysis.

7.8 mm in diameter, were machined out from the tiles. Fig. 2 shows schematically the sampling procedure whereas all technical details can be found in [8,9]. This procedure allowed the decrease of the total radioactivity level to be handled in further studies ( $1 \times 10^{16}$  T cm<sup>-2</sup> corresponds to radioactivity of 17.8 MBq) aiming at the comparative determination of D and T and the distribution of isotopes in the surface layer and in the bulk. Therefore, the samples had to be machined from very adjacent locations because the distribution of co-deposited material is known to be highly non-uniform [6,10–15]. The samples for T analysis were sliced into 1 mm discs, then fully combusted and the tritium content was determined in tritiated water [9].

In the second set of samples the amount and distribution of deuterium, beryllium and carbon in co-deposits was determined by means of nuclear reaction analysis (NRA). It was based on target irradiation with a 2.5 MeV <sup>3</sup>He<sup>+</sup> beam and detection of protons produced in the following reactions: <sup>3</sup>He(d,p)<sup>4</sup>He, <sup>3</sup>He(<sup>9</sup>Be,p)<sup>11</sup>C, <sup>3</sup>He(<sup>12</sup>C,p)<sup>14</sup>N. The information depth for detecting D is around 7–9 μm, i.e. greater than the deposit thickness on most of the samples, but much smaller than the thickness of 1 mm in which the total amount of tritium was traced. It has previously been shown that both D [16,17] and T [9] migrate into the bulk of carbon fibres and graphite. Therefore, especially in case of very thick co-deposited layers and large contents of hydrogen isotopes, the comparison of D and T has, to some extent, rather qualitative character because of the different layer thickness analysed using full combustion and NRA methods.

### 3. Results and discussion

In this section we first give an overview of surface morphology for samples originating from the central part of the tiles (one sample per tile). This is followed by a detailed description of results for surfaces located in the corner of the inner divertor, i.e. tiles 3 and 4, where

the greatest inhomogeneity of the poloidal distribution of species has been observed.

Plots in Fig. 3(a) and (b) show a poloidal distribution of the species: D, Be, T whilst in Fig. 3(c) the Be-to-C ratio is given. The results reveal significant asymmetry in the erosion–deposition pattern. The limiter surfaces are characterised by relatively small content of beryllium and hydrogen isotopes. Very low values of the Be-to-C ratio clearly indicate that the regularly evaporated beryllium coating (one evaporation per week with the average coating of  $5 \times 10^{16}$  Be cm<sup>-2</sup>) has effectively been eroded from the graphite limiters and transported downwards to the inner divertor channel. Small amounts of deuterium in the main chamber (mostly below  $1 \times 10^{18}$  cm<sup>-2</sup>) are most probably attributed to a shallow implantation of this species. There is no indication of a thick co-deposit formation. Carbon and beryllium are found in a fairly uniform mixed layer as inferred from the NRA spectra. No shift in positions of proton peaks (from <sup>3</sup>He–<sup>12</sup>C and <sup>3</sup>He–<sup>9</sup>Be reactions) on energy scale was observed when the Be and C features in spectra for co-deposits and pure elements are compared. Therefore, one concludes that erosion of both elements occurs simultaneously and from the same locations on the wall. A question regarding the contribution of ions and neutrals to the overall erosion rate remains to be answered.

The above mentioned facts confirm previous other findings that the wall main chamber wall is the erosion dominated area and the source of beryllium and carbon impurities. The statement is strongly supported by the flux measurements with fast reciprocating Mach [10] and surface collector [18] probes detecting the preferential flow direction of the deuterium background plasma (Mach number ~0.5) and impurities towards the inner divertor leg where, indeed, the deposition is concentrated. This direction of carbon migration has very recently been proven in experiments with the injection of the <sup>13</sup>CH<sub>4</sub> transport marker into the main chamber. Significant amounts of injected C-13 were found deposited on the inner divertor tiles [19]. The composition of films deposited on plasma facing surfaces of tiles 1–4 is dominated by the presence of beryllium (high Be-to-C ratio). Moreover, these films contain significantly more Be and D than detected in co-deposits in the base and in the outer divertor where the distribution of those species is fairly uniform. The beryllium concentration on tile 3 may be even underestimated since the film thickness is greater than the analysis depth for this element.

The distribution of tritium follows that of deuterium but the D-to-T ratio ranges from 40 to 140 when the isotope contents in respective locations are compared. Indeed, the values exceeding 50 could be expected from: (i) the overall ratio of gas input, D:T around 50, during the entire operation period when the tiles were in the machine (DTE-1 campaign with the D:T around 1 was only a part of this period), (ii) the tritium clean-up

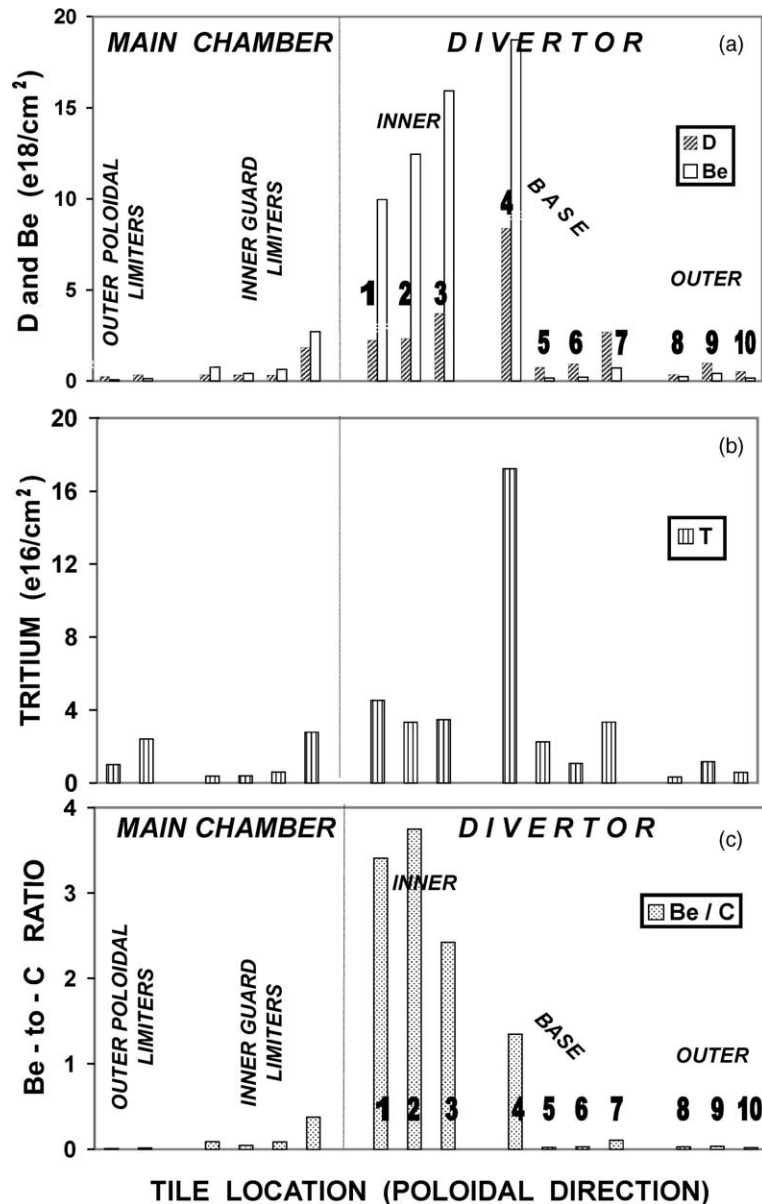


Fig. 3. Concentration and relative distribution of species on plasma facing surfaces in the main chamber and the divertor: (a) deuterium and beryllium, (b) tritium, (c) beryllium-to-carbon ratio.

procedure after the DT experiments. The two isotopes were analysed in layers of different thickness and in samples originating from very adjacent but not the same location (see Section 2 and Fig. 2). This may be the reason for a certain scatter of the  $C_D/C_T$  values because of a non-homogeneous deposition pattern on the tiles. Secondly, a different rate of in-depth migration of D and T into the CFC bulk cannot be excluded and it may also play a certain role.

Detailed results for all samples from the corner tiles (3 and 4) are shown in Fig. 4. Drastic differences are

noted when the morphology of plasma facing and shadowed regions is compared. The most striking is a concentration threshold of both D and Be upon the transition between the zones: the deuterium concentration sharply rises (the same observed for tritium) whereas the beryllium content significantly decreases (samples 3d and 4b) and then drops (samples 3e and 4a) below the detection limit for Be with the NRA method ( $1 \times 10^{17} \text{ cm}^{-2}$ ). It gives a strong indication that hydrogen isotopes accumulated in the shadowed region are embedded in thick and flaking carbon films.

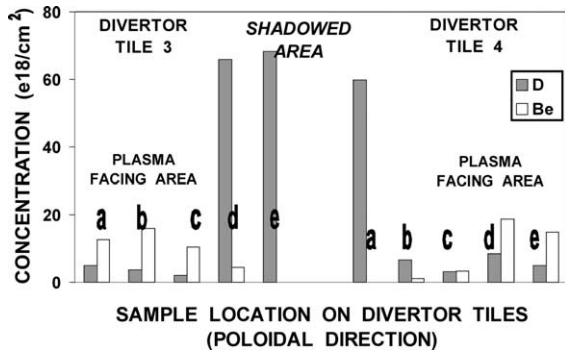


Fig. 4. Distribution and concentration of deuterium and beryllium on tiles 3 and 4 of the divertor. Notation of samples 'a'–'e' denotes the sequence of samples along the poloidal direction. On tile 3, sample 'a' is located on top of the tile and sample 'e' in the shadowed region of the inner divertor. On tile 4, the notation starts in the shadow region ('a') and continues towards tile 5.

Ion induced detrapping of D with a  $^3\text{He}^+$  beam [20] allows some conclusions regarding the film properties based on the deuterium-to-carbon concentration ratio. As inferred from detrapping measurements, the layers belong to a category of 'soft' films [21] as they are characterised by a high  $C_D/C_C$  ratio exceeding 0.5. It is also known that release rates for  $\text{C}_2\text{H}_x$  hydrocarbons from such layers are high at elevated temperatures [22]. The initial detrapping efficiency reaches  $700 \text{ D}/^3\text{He}^+$  for films from the deposition zone (tile 3) in comparison to a much smaller D release rate determined for species implanted into CFC limiters being in the erosion dominated areas (features resembling 'hard' films). The plots for deuterium release for films formed in different locations are presented in Fig. 5 whereas the data in Table 1 show the overall D-detrapping efficiency (normalised for the  $^3\text{He}^+$  dose of  $1.8 \times 10^{16} \text{ cm}^{-2}$ ) from film with different initial contents of D and Be. The data clearly indicate the film properties depend on the place of its formation and corresponding temperature specific for a given location. Other factors, such as beryllium concentration and initial fuel content have only minor influence to the release efficiency of deuterium.

These meaningful differences in the Be, C and D distribution are attributed to the differences in physics underlying the erosion of both elements (Be, C) and their transport to and in the divertor region. Beryllium is only physically sputtered because it does not react with hydrogen isotopes towards the formation of volatile compounds. The experimentally and theoretically determined sputtering threshold of Be by D projectiles (either ions or neutrals) is about 18 eV and, as a consequence, Be coating can efficiently be removed from the limiters. The results (see Fig. 3) indicate that beryllium deposition in the inner divertor reflects the amounts of this element transported in the SOL and then deposited

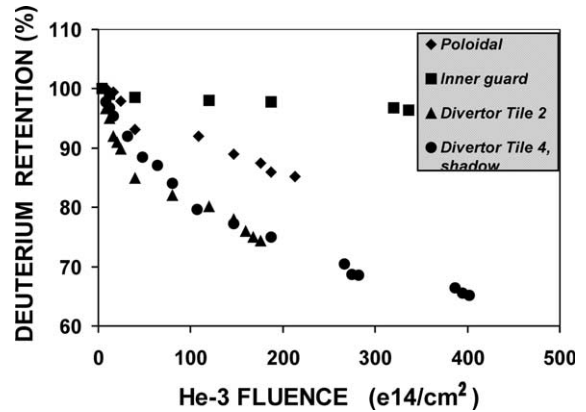


Fig. 5. Characteristics of  $^3\text{He}$ -induced detrapping of deuterium from co-deposits on the limiter and divertor tiles.

Table 1

Characteristics of  $^3\text{He}$ -induced detrapping of deuterium from co-deposits on the limiter and divertor tiles

Tile location	Amount detrapped (%)	$C_D$ initial ( $10^{18} \text{ cm}^{-2}$ )	$C_{Be}$ ( $10^{18} \text{ cm}^{-2}$ )
Poloidal limiter	14.1	1.74	1.54
Inner guard limiter	2.1	3.90	2.02
Divertor, tile 2	26.1	3.80	3.51
Divertor, tile 4 (shadow)	25.6	35.05	0

Data normalised for a  $^3\text{He}^+$  dose of  $1.8 \times 10^{16} \text{ cm}^{-2}$ .

on the vertical target. Some re-erosion of Be may still occur until the temperature of incoming ion flux is still above 4–5 eV.

Carbon deposited in the divertor also originates from the main chamber wall. Its erosion is mainly driven by the formation of hydrocarbon even under the impact of low energy species [23]. The reaction efficiently occurs in presence of the cold divertor plasma when temperatures are in the range from 5 to 20 eV [24]. Therefore, the re-deposited carbon films can be either easily eroded by further hydrogen impact or dissociate thermally into a large variety of hydrocarbons. This shows up in JET spectroscopically in a very large apparent yield of hydrocarbon formation reaching values greater than 10% in the inner divertor [25]. Carbon can be eroded by this process repeatedly and hydrocarbon molecules may thus travel long distances until being finally re-deposited in remote areas. This occurs on cold surfaces either on shadowed parts of the tiles or on water-cooled louvers where the formation of thick and fuel-rich carbon films has been proven [10,26]. Fuel accumulation in those areas is clearly associated with carbon transport and its re-deposition. The inner target thus acts only as an

intermediate step for carbon incoming from the main chamber.

#### 4. Conclusions

The study of relative distributions of beryllium, carbon and fuel species on the limiter and divertor tiles from the DTE-1 campaign at JET shows a large asymmetry in the distribution of elements. This is caused by the preferential flow of the deuterium background plasma driving impurities towards the inner divertor leg. Our results suggest that beryllium and carbon are eroded from the inner wall of the main chamber and they are predominantly transported to the inner divertor. Carbon then undergoes mainly chemical erosion and migrates into the shadowed areas leaving behind a layer which is dominated by beryllium. The low plasma temperatures in the inner divertor prevent the erosion of this layer and very little beryllium is seen in areas shadowed from the plasma. An important implication of these observations is that, in a machine with an all beryllium first wall in the main chamber, fuel retention may be significantly reduced due to removal of the carbon source.

#### Acknowledgement

This work has been conducted under the European Fusion Development Agreement.

#### References

- [1] M. Keilhacker, M.L. Watkins, JET Team, *J. Nucl. Mater.* 266–269 (1999) 1.
- [2] D. Stork (Ed.), *Technical Aspects of Deuterium–Tritium Operation at JET (special issue)*, *Fusion Eng. Des.* 47 (1999).
- [3] P.R. Thomas, JET Team, *J. Nucl. Mater.* 176&177 (1990) 3.
- [4] A.T. Peacock et al., *J. Nucl. Mater.* 176&177 (1990) 326.
- [5] G. Kalinin et al., *Fusion Eng. Des.* 55 (2001) 231.
- [6] J.P. Coad, P.L. Andrew, A.T. Peacock, *Phys. Scr. T* 81 (1999) 7.
- [7] A.C. Rolfe, *Fusion Eng. Des.* 36 (1997) 91.
- [8] R.-D. Penzhorn et al., *Fusion Eng. Des.* 56&57 (2001) 105.
- [9] R.-D. Penzhorn et al., *J. Nucl. Mater.* 288 (2001) 170.
- [10] J.P. Coad et al., *J. Nucl. Mater.* 290–293 (2001) 224.
- [11] J.P. Coad, M. Rubel, C.H. Wu, *J. Nucl. Mater.* 241–243 (1997) 408.
- [12] M. Rubel, P. Wienhold, D. Hildebrandt, *J. Nucl. Mater.* 290–293 (2001) 473.
- [13] P. Wienhold et al., *Phys. Scr. T* 81 (1999) 19.
- [14] C. Skinner et al., *J. Nucl. Mater.* 290–293 (2001) 486.
- [15] C. Skinner et al., *J. Nucl. Mater.* 241–243 (1997) 214.
- [16] B. Emmoth, M. Rubel, E. Franconi, *Nucl. Fusion* 30 (1990) 1140.
- [17] M. Rubel et al., *J. Nucl. Mater.* 196–198 (1992) 285.
- [18] M. Rubel et al., *Proceedings of the 28th EPS Conference on Plasma Physics and Controlled Fusion*, Funchal, Portugal, June 2001, *Europhysics Conference Abstracts* 25A (2001) 1609.
- [19] J.P. Coad et al., these Proceedings. [PII: S0022-3115\(02\)01403-4](#).
- [20] M. Rubel, H. Bergsäter, P. Wienhold, *J. Nucl. Mater.* 241–243 (1997) 1026.
- [21] W. Jacob, *Thin Solid Films* 326 (1998) 1.
- [22] A. von Keudell et al., *Nucl. Fusion* 39 (1999) 1451.
- [23] V. Philipps et al., *Vacuum* 67 (2002) 399.
- [24] S.K. Erents et al., *Nucl. Fusion* 40 (2000) 295.
- [25] M. Stamp et al., *Phys. Scr. T* 91 (2001) 13.
- [26] J.P. Coad et al., *Proceedings of the Eighth European Conference on Application of Surface and Interface Analysis (ECASIA'99)*, Seville, Spain, October 1999.